Chihyu Chen

Final Report

# Understanding Cabling Noise in LIGO

**Abstract.**

Test masses and other key optics in LIGO are supported as pendulums to filter out noise from ground motion, and in the forthcoming AdvLIGO upgrade, these will be multistage pendulums. Some of them need to be fitted with multiple channels of sensors and actuators. The cabling that needs to be run between the levels may be stiff and heavy and can potentially degrade the vibration isolation or create thermal noise.[1] In order to understand the cabling noise, we developed an apparatus that characterizes the cabling used in the double pendulum suspension for the OMC for its spring constant and damping function. For the pitch motion of the pendulum, we found the cabling's torsion spring constant to be $k_{tor}$ = 0.005±0.002 N-m/rad, its bending spring constant to be $k_{bend}$ = 4.9±0.7 N/m, and that the cabling exhibits structural damping with a constant damping function of $\Phi$ = 0.003±0.001 .

## Introduction

The Laser Interferometer Gravitational-Wave Observatory (LIGO), is a ground based laser Michelson interferometer (Figure 1[2]) that searches for gravitational waves by detecting, effectively, the change of length in the detector's perpendicular cavities. When gravitational waves interact with the test masses, the test mass displacement is in the order of $10^{-19}$ m. Ground vibration, on the other hand, moves in the order of $10^{-6}$m. Thus, the test masses, on which the interferometer mirrors are coated, are suspended as a part of multi-stage pendulum from an actively isolated platform, to isolate against seismic noise.

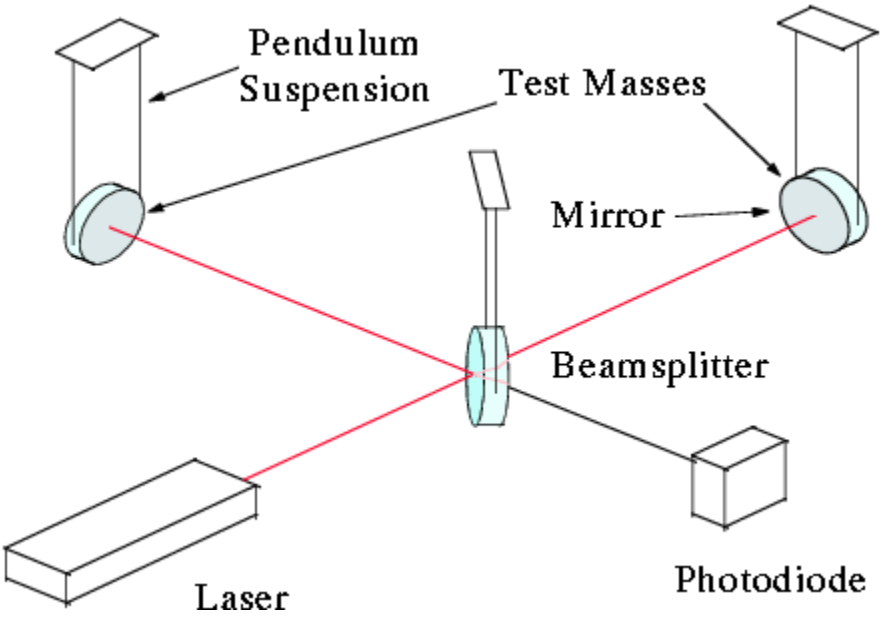


**Figure 1. A schematic of LIGO as a laser Michelson Interferometer that has it's mirrors coated on test masses, which in turn are suspended as pendulums to isolate against the ground motion.**

Some of these suspended objects need to be fitted with multiple channels of sensors and actuators. With one end on a pendulum stage and the other attached to the grounded support structure, the cabling provides a direct path for the ground motion to be injected into the suspension. The cabling may be relatively stiff and heavy and therefore can potentially degrade the vibration isolation or create thermal noise.

We studied the effects of cabling used in the double pendulum suspension for the OMC by experimentally characterizing the cabling for its spring constant and damping function, and constructing a computer model (done by Julian Freed-Brown, based on Mathematica tool packages by Mark Barton) that uses these measurements to quantify the isolation deterioration. This paper will present primarily on the characterization of the cabling.

**Types of Damping[3,4]**

Since we believe that the main contribution to the suspension's degradation would come from the damping in the cabling, the primary goal of our experiment is to characterize the damping.

The two most common types of damping are velocity damping and structural damping. Assuming velocity damping, the damping is modeled as retarding force that is proportional to the velocity of the mass "m", $F_d = -cv$. Applying Newton's second law on the mass, we get:

$$m\ddot{x} + c\dot{x} + kx = F \qquad \text{eq. 1}$$

When the system is left alone to damp down, F = 0, and we have

$$m\ddot{x} + c\dot{x} + kx = 0 \qquad \text{eq. 2}$$

On the other hand, if we assuming structural damping, this free damped vibration of eq.2 would have its damping modeled as a force proportional to the displacement but in phase with the velocity. The resulting equation of motion is:

$$m\ddot{x} + k(1 + \phi)x = 0 \qquad \text{eq .3}$$

Where Φ, the damping function, is the fraction of energy lost in each cycle of the vibration. Φ(f) as a function of frequency f is informative because it allows us to unambiguously distinguish between velocity and structural damping:

$$\phi = \text{const} \qquad \text{eq. 4} \qquad \text{[structural damping]}$$

$$\phi \propto f \qquad \text{eq.5} \qquad \text{[velocity damping]}$$

**Determination of the Cabling Damping Function $\Phi_c(f)$ and Torsion Spring Constant $k_{Ctor}$**

Consider a test pendulum in suspension with cabling symmetrically attached to both of its sides, as shown in Figure 2, with the left side being our experimental apparatus and the right side being a schematic of it.

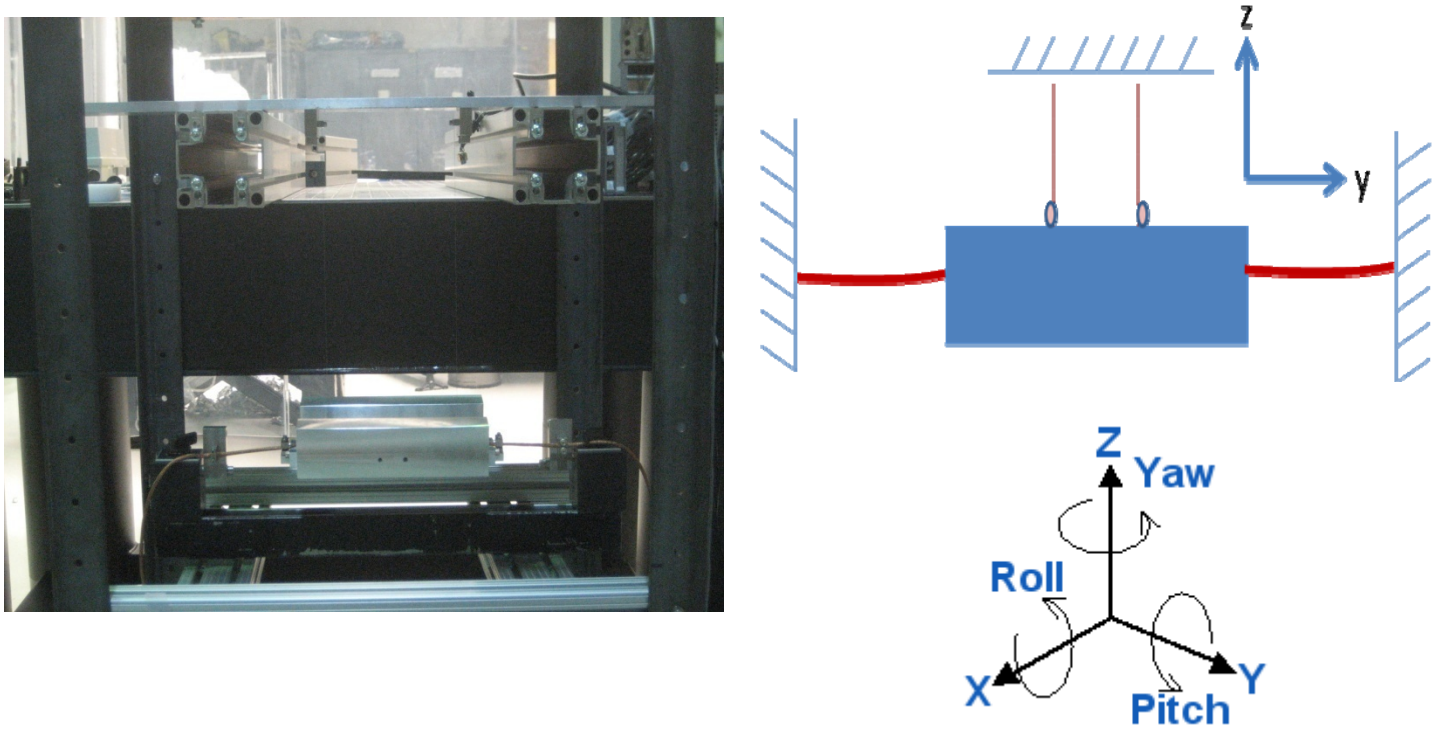


**Figure 2. (*left)* The two wire torsion pendulum in suspension, with two wires attached on each side. (*right*) A schematic of the set up. (*bottom right*) Definition of the pendulum's angular displacements.**

Analyzing the yaw motion as an example, the complex spring constant of eq 3, k(1+iΦ) for the combined system of the pendulum and the cabling can be written as:

$$k_T\,(1 + i\phi_T) = k_P\,(1 + i\phi_P) + k_C\,(1 + i\phi) \qquad \text{eq. 6}$$

Where the subscript "P" stands for the pendulum, "C" stands for the cabling, and "T" stands for the effective values for the combined system.

Knowing that the pendulum has very low damping compared to cabling, we can set $\Phi_p = 0$ .

$$k_T\,(1 + i\phi_T) = k_P + k_C\,(1 + i\phi) \qquad \text{eq. 7}$$

and with some algebraic manipulation:

$$\phi_T = \frac{k_C\,\phi_C}{k_C + k_P} = \frac{k_C\,\phi_C}{k_T} \qquad \text{eq. 8}$$

where

$$k_T = k_C + k_P \qquad \text{eq. 9}$$

Now, given that the angular spring constant k can be generically expressed as

$$k = If^2 \qquad \text{eq. 10}$$

we see that,

$$I_T f_T^2 = I_P f_P^2 + I_C f_C^2 = k_T \qquad \text{eq. 11}$$

Substituting this result back into eq. 8, we get

$$\phi_T = \frac{k_C \phi_C}{I_T f_T^2} \qquad \text{eq. 12}$$

When conducting this experiment, we set the pendulum in the yaw direction resonant frequency mode, and then measure both the resonant frequency $f_T$ and Q, the quality factor at the resonant frequency, which can be related to eq 12. through the following:

Since for our system the dominant mechanical loss is through the dominant elastic element (the cabling),

$$Q_T(f_T) = \frac{1}{\phi_T(f_T)} \qquad \text{eq .13}$$

Where $Q(f_T)$ is the quality factor at the resonant frequency $f_T$ of the torsional pendulum. Substituting eq. 13 into eq.12, we have,

$$Q_T(f_T) = \frac{f_T^2 I_T}{k_C \phi_C} \qquad \text{eq. 14}$$

$Q_T$ and $f_T$ are measured in the experiment, $I_T$, can be calculated analytically, and $k_C$ can also be computed provided that we make the experimental measurements of $f_P$, the pendulum's resonant frequency before attaching the cabling, and $f_T$, the pendulum's resonant frequency after attaching the cabling. The calculation is as follows:

Rearranging eq. 11, we have

$$I_C f_C^2 = k_C = I_T f_T^2 - I_P f_P^2 \qquad \text{eq. 15}$$

We note that the inertia of the cabling is negligible as compared to the pendulum, and therefore the inertia of the combined system, $I_T$, would be approximately equal to the inertia of the pendulum alone, $I_P$. As a result we have,

$$k_C = I_p \left(f_T^2 - f_P^2\right) \qquad \text{eq. 16}$$

Where we first measure the pendulum's resonant frequency, $f_P$, and then attach the cabling, and finally measure the resonant frequency of the combined system, $f_T$.

With $k_C$ also determined, we can find $\Phi_c$ using eq. 14.

Referring back to equations 4 and 5, we see that if the cabling exhibits velocity damping, then a plot of $Q_T^{1/2}$ vs $f_T^{1/2}$ would give a curve which varied as a function of $f_T^{1/2}$ ; if the cabling exhibits structural damping, then this plot would yield a straight line through the origin.$Q_T$, the quality factor of the combined system measured at its resonant frequency $f_T$, are measured quantities as discussed previously.

**Determination of the Cabling's Bending($k_{Cbend}$ ) Spring Constant, Bending Modulus of Elasticity($E_{bend}$) and its Torsion($k_{Ctor}$ ) Spring Constant.**

The cabling's bending spring constant $k_{Cbend}$ and modulus of elasticity($E_{bend}$) can be estimated by cantilevering a section of the cabling off a clamp( Figure 3), and considering the bending equations of a uniform cantilevered beam.

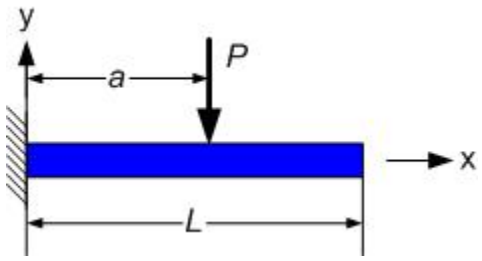


**Figure 3. The cantilever beam showing the load P applied at distance a from the support.**

The beam deflects downwards when acted upon by a downwards force P. Let this force act on the tip of the beam, and let the tip deflection be $\delta$, then we can find the bending spring constant

$$k_{bend} = \frac{P}{\delta} \qquad \text{eq. 17}$$

And the bending modulus of elasticity is

$$E_{Cbend} = \frac{P}{\delta}\frac{L^3}{3\,I_{cab}} = k_{Cbend}\frac{L^3}{3\,I_{cab}} \qquad \text{eq. 18}$$

Where $I_{cab}$ is the area moment of inertia or the cabling, and is given by:

$$I_{cab} = \frac{\pi r^4}{4} \qquad \text{eq. 19}$$

and r is the radius of the cabling.

The cabling's torsion spring constant $k_{Ctor}$ can be estimated by clamping something heavy to a piece of cabling, and suspending combination as a torsion pendulum where the pendulum's bob is the clamp. The pendulum's frequency is given by:

$$\omega^2 I = (2\pi f)^2 I = k_{Ctor} \qquad \text{eq. 20}$$

Where I is the mass moment inertia of the pendulum. Since the inertia of the cabling is much smaller than that of the clamp, we can take I to be $I_{clamp}$. Hence:

$$(2\pi f)^2 I_{clamp} = k_{Ctor} \qquad \text{eq. 21}$$

**Methods**

The cabling (Figure 4) used in these experiments consists of 18 electrical wires inside a copper sheath (as opposed to the black PEEK sheath). The cabling has a linear mass density of 0.32g/cm and a diameter of 4mm. About 90 cm of this cabling was manufactured. It was then cut in half. Finally, the effective length of each half was made arbitrarily shorter by clamping, so that what is behind the clamp can be assumed to have no effect on what is in front of it. For the two wire test pendulum experiment (Figure 2), the effective cabling length was about 7cm on each side. For the cantilevered cabling experiment, the effective cabling length was 5 cm.

These parameters are chosen to resemble the cabling used in the OMC, where two such cabling enters the OMC cage through the top, and halfway to the OMC bench, each of the two 18-wire cables split into two 9-wire cables. It is the 4 smaller 9-wire cables that are connected to the OMC bench.

The apparatus, data collecting and analysis methods, are discussed separately for the two wire test pendulum, the cantilevered cabling, and the cabling-clamp torsional pendulum in the following subsections.

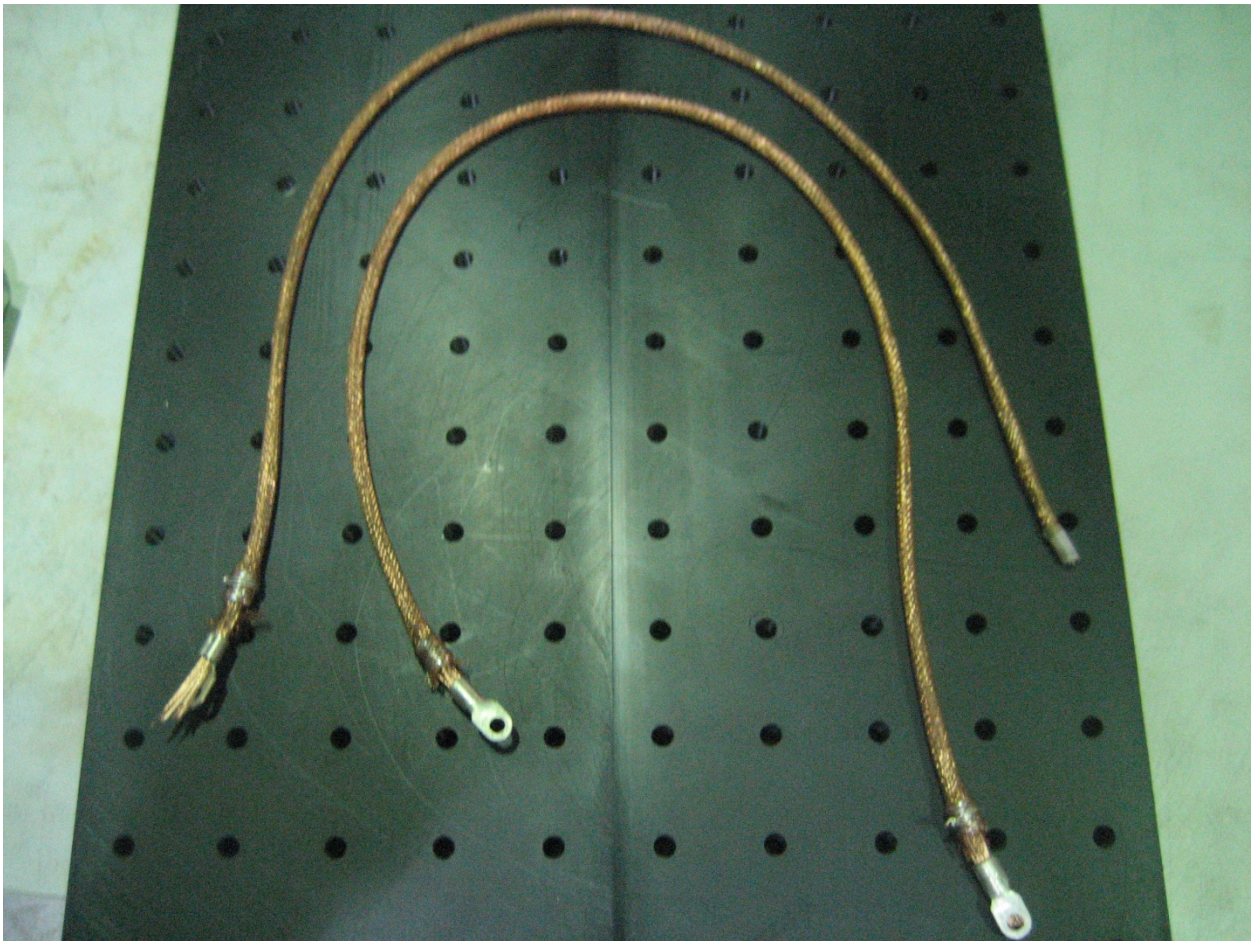

**Figure 4. The cabling used in our experiments. Two such cablings are used in the OMC double pendulum suspension.**

## The Two Wire Test Pendulum Experiment

The design of the test pendulum

To ensure that we can check for the frequency dependence of $\Phi_c$ , the ability to vary the pitch and yaw frequencies over about an order of magnitude range of frequencies was a major design goal. Figure 5 is a schematic of our test pendulum, with the two frequency varying parameters "n" and "d" defined.

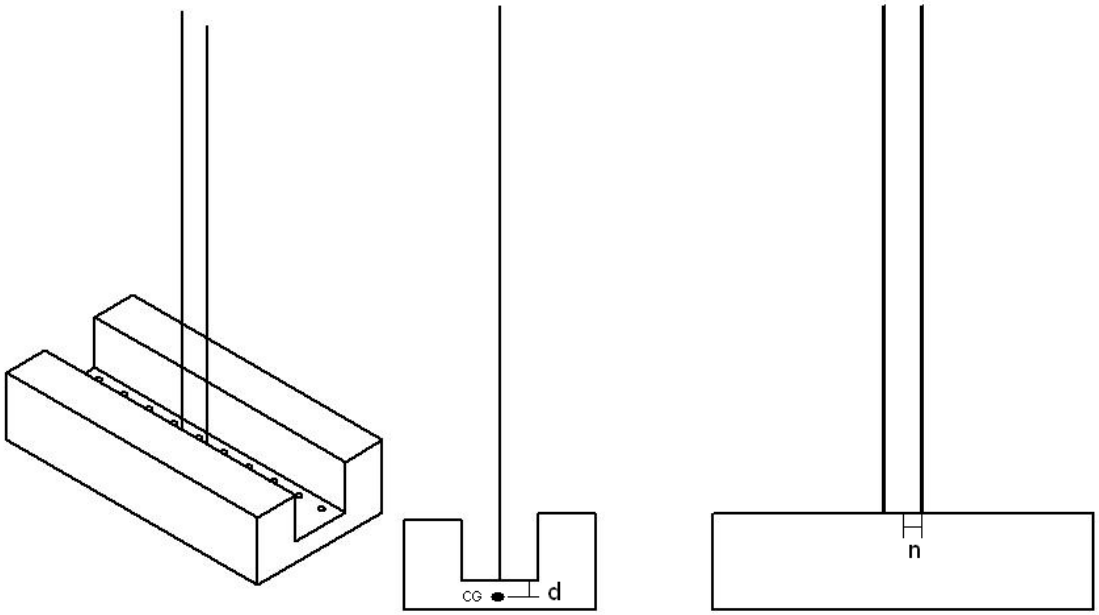


**Figure 5. A schematic of the present design of our Q-test torsional pendulum. The parameters "d" and "n" as defined in the paragraph are labeled here.**

"n" determines the pendulum's yaw frequency, and is varied by clamping the suspension wires symmetrically along the column of screw holes as shown in the left most picture in Figure 5. "d" determines the pendulum's pitch frequency, and is varied by inserting plates into the middle trough, as shown in Figure 6, to raise the height of the suspension wire attachment.

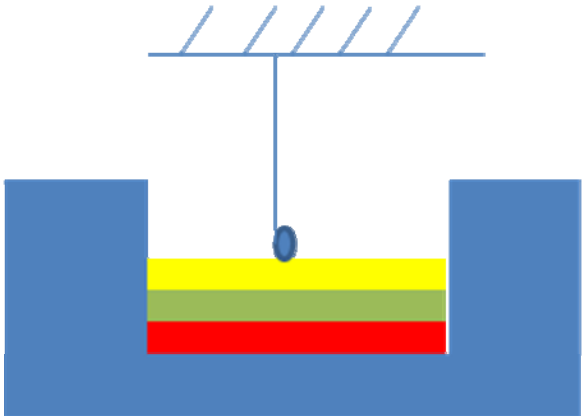

**Figure 6. Schematic showing three plates inserted in the center trough region of the pendulum. This is done to vary the "d" distance, which determines the pendulum's pitch frequency.**

The dimensions of the test pendulum is 10cm wide * 20cm long* 5cm tall. Both the pendulum and the plates are made of aluminum.

Data Collection

A Kaman displacement sensor is used to measure the ring down of the pendulum. The Kaman sensor induces an eddy current in a metallic surface, then detects the magnetic field from the eddy current, and outputs a voltage that is proportional to the distance between the metallic surface and the sensor. The time varying voltage is recorded by the LabVIEW data logging system for later analysis.

Data Analysis

A typical ring down taken by the Kaman sensor is shown in Figure 7.

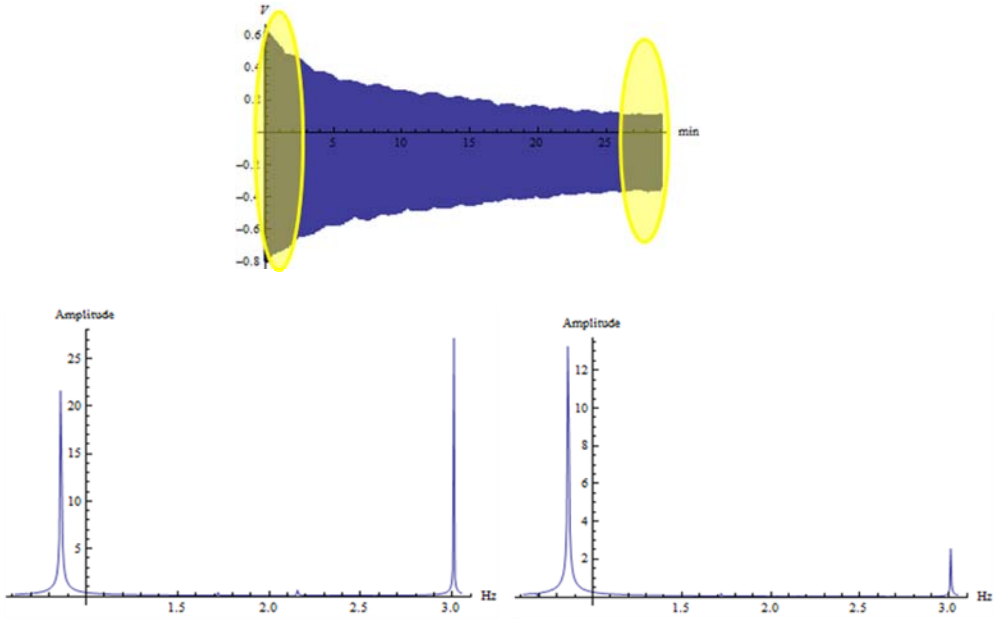


**Figure 7. (Top) A typical ring down taken from the Kaman sensor. The circled ends represent chunks of data that are taken out of the beginning and the end of the ring down. (Left and Right) The chunks of data Fourier transformed into frequency space.**

Mark Barton wrote a program that takes chunks (circled in Figure 7) of data out of the beginning and end of the ring down, then Fourier transform them into frequency space, as shown in the left and right spectrum in Figure 7. Although during the experiment only one mode was meant to be excited, we usually end up exciting at least one other mode, and hence there are two peaks in the spectrum. The peak of interest is identified, and a comparison of the peak amplitudes at the beginning and at the end of the ring down would yield the quality factor Q for the ring down.

## The Cantilevered Cabling Experiment

In simulating a cantilevered beam, the cabling clamp shown in Figure 2 is clamped on to one end of a segment of cabling, such that 5 cm of cabling is cantilevered off the clamp. Then, three different washers weighing 3, 7, and 12 grams are sequentially hung near the tip of the cabling. Finally, the tip displacement is measured and recorded in Table 1.

Table 1. Data recorded for the cantilevered cabling experiment. Two trials are repeated for each load washer. For each washer, the cabling tip deflection is found for each trial, the average is calculated, and then the bending spring constant $k_{Cbend}$ is computed.

| mass | 3 grams | | | | |
|---|---|---|---|---|---|
| trial | original pos (mm) | end pos(mm) | deflection(mm) | avg defl (mm) | $k_{Cbend}$(N/m) |
| 1 | 205 | 210 | 5 | 6 | 4.9 |
| 2 | 205 | 212 | 7 | | |
| mass | 7 grams | | | | |
| trial | original pos (mm) | end pos(mm) | deflection(mm) | avg defl (mm) | $k_{Cbend}$ (N/m) |
| 1 | 205 | 222 | 17 | 16 | 4.3 |
| 2 | 205 | 220 | 15 | | |
| mass | 12 grams | | | | |
| trial | original pos (mm) | end pos(mm) | deflection(mm) | avg defl (mm) | $k_{Cbend}$ (N/m) |
| 1 | 205 | 226 | 21 | 21 | 5.6 |
| 2 | 205 | 226 | 21 | | |

For each trial the cabling bending spring constant is calculated by eq 17. These values are then averaged to give the estimate:

$$k_{Cbend} = \frac{1}{3}(4.9 + 4.3 + 5.6) = 4.9 \pm 0.7 \frac{N}{m}$$

where the error is taken as 1 standard deviation of the three $k_{Cbend}$ calculations, one for each washer.

To find the cabling's bending modulus of elasticity $E_{Cbend}$, we compute $I_{cab}$ as given in eq. 19, and substitute the results into eq. 20. We end up with $I_{cab} = 1.2566*10^{-11}$ m, and

$$E_{Cbend} = \frac{4.9 * 0.05^3}{3 * 1.2566 * 10^{-11}} = 1.6 * 10^7 \text{ Pa}$$

## The Cabling-Clamp Torsion Pendulum Experiment

The Cabling-Clamp torsion pendulum is constructed by first placing one end of the cabling in between two aluminum blocks, and then screwing the blocks together, thereby clamping the cabling in place. Suspend this combination from its top, and we have a torsion pendulum. The pendulum is given an angular displacement and then allowed to oscillate. The ringdown data for four trials is given in Table 2.

Table 2. The recorded data for the Cabling-Clamp torsion pendulum ringdown. For each of the 4 trials, the number of cycles and the corresponding time elapsed is recorded. Frequency is then calculated, and averaged over the trials. Finally, and estimate of the torsion spring constant $K_{Ctor}$ is also provided.

| Trial | # of periods | time(sec) | f(Hz) | favg (Hz) | $k_{Ctor}$ (N) |
|---|---|---|---|---|---|
| 1 | 4 | 3.13 | 1.277955272 | 1.11679659 | 0.003046 |
| 2 | 5 | 4.89 | 1.022494888 | | |
| 3 | 4 | 3.87 | 1.033591731 | | |
| 4 | 4 | 3.53 | 1.133144476 | | |

$k_{Ctor}$ is calculated according to eq. 21. $I_{clamp}$ is the mass moment of inertia of the two blocks with respect to the axis of the cabling, and is calculated to be $6.19*10^{-5}$ kg-$m^4$, based on the measurement that each block has the dimensions of 13mm*26mm*50mm, and the gap between the blocks where the cabling fits is 3mm, and that the mass of the block is 108 grams.

$k_{Ctor}$ is estimated to be:

$$k_{Ctor} = 0.003 \frac{N \cdot m}{rad}$$

### Results

As part of the two wire torsion pendulum experiment, we computer modeled the two wire torsion pendulum (without the cabling) shown in Figure 2, and predicted its frequencies in various degrees of freedom. Table 3 compares the measured frequencies against the predicted values.

Table 3. A comparison between the measured and predicted pendulum frequencies for the yaw and pitch angular displacement. "n" and "plate" are parameters of the test pendulum that varies the pendulum frequencies. Please see the Methods section for details.

Yaw mode

| | frequency (Hz) | |
|---|---|---|
| | measured | predicted |
| n=1 cm | 0.134 | 0.1366 |
| n=3 cm | 0.4089 | 0.4098 |
| n=5 cm | 0.6836 | 0.683 |
| n=7 cm | 0.958 | 0.956 |
| n=9 cm | 1.227 | 1.229 |

Pitch mode

| | frequency (Hz) | |
|---|---|---|
| | measured | predicted |
| 0 plate | 0.656 | 0.414 |
| 1 plate | 1.56 | 1.458 |
| 2 plates | 2.14 | 2.066 |
| 3 plates | 2.61 | 2.559 |
| 4 plates | 3.01 | 2.97 |

As shown, the predicted yaw frequencies are highly accurate, and the predicted pitch frequencies are fair, when compared to the measurements.

For the pitch mode, we measured $Q_T$ for various frequencies, and plotted $Q_T^{1/2}$ v.s. f as shown in Figure 8. Within experimental error, this is a straight line through the origin. According to the previous section, this unambiguously concludes that for the pendulum's pitch mode, the cabling exhibits structural damping.

By computing $k_C$ and $\Phi_C$ for each of the frequencies tested, and finding the standard deviations, we find that for the pitch mode of the pendulum $k_C = 0.005 \pm 0.002$ N-m/rad and $\Phi_C = 0.003 \pm 0.001$, which is constant with respect to f. It is important to note that during the pitch mode of the pendulum, the cabling is actually being twisted about its long axis, so the $k_C$ obtained in this experiment is the cabling's torsion spring constant.

In a different experiment, the cabling-clamp torsion pendulum experiment, we estimated the torsion spring constant of the cabling's torsion spring constant $k_{Ctor} = 0.003$ Nm/rad , which agrees well with the value $k_C = 0.005 \pm 0.002$ N-m/rad found in the two wire torsion pendulum experiment.

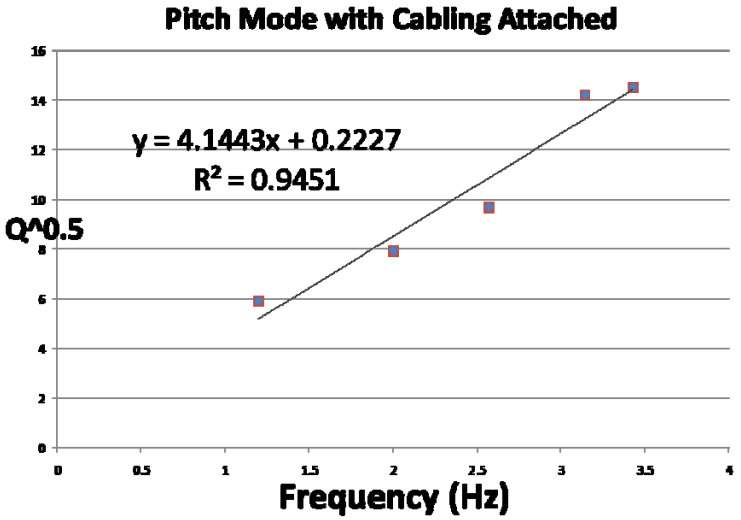


**Figure 8. $Q_T^{1/2}$ v.s. f for the pitch mode. Within experimental error, this is approximately a straight line through the origin, therefore concludes that the cabling exhibits structural damping in the pitch mode.**

Finally, in the cantilevered cabling experiment we estimated the cabling's bending spring constant $k_{Cbend}$ = 4.9 N/m. This experiment was inspired by the work of Dennis Coyne[5], and in his experiment he estimated the spring constant of his cabling to be about 8.1 N/m. This result is surprising, since Coyne's cabling had only a single pair of twisted wires, while ours has 18 wires. Thus if the wires contribute significantly to $k_{Cbend}$, our cabling's bending stiffness should be greater, not less than that used by Coyne. We provide a possible explanation for this discrepancy in the next section.

We still note that the $k_{Cbend}$ of our is in the same order of magnitude as that of Coyne's, and that our estimate of the cabling's bending modulus of elasticity $E_{Cbend} = 1.6*10^7$ Pa is in the same order of magnitude of his calculated value for his cabling, $E = 9.3*10^7$ Pa.

**Discussion**

While in the modeling we have paid attention to such detail as the change in position of the pendulum's center of gravity with the successive insertion of plates into the trough region, the experimentally measured pitch frequencies don't agree well with the modeling predictions. This is probably due to the fact that the pitch frequencies are very sensitive to the attachment point of the suspension wires on the pendulum. Although we designed for the suspension wires to be symmetrically placed along the center of the length of the "trough" of our pendulum, in practice this attachment point is very difficult to place accurately. However, the great agreement between the model and the experiment for the yaw frequency gives us confidence on the modeling equations, which are formulated by Calum Torrie, and are also used in other models of LIGO's suspensions.

Also, the good agreement of the torsion spring constant of the cabling found across two independent experiments, the two wire torsion pendulum experiment and the cabling-clamp torsion pendulum experiment, gives us confidence that the value $k_{Ctor} = 0.005 \pm 0.002$ N-m/rad for the torsion spring constant is of the correct order of magnitude.

The disagreement between our measurement of our cabling's bending stiffness (4.9 N/m) and Coyne's measurement of his cabling stiffness (8.1 N/m) is puzzling. Coyne's cabling had only a

single pair of twisted wires, while ours has 18 wires. Thus if the wires contribute significantly to $k_{Cbend}$, our cabling's bending stiffness should be greater, not less than that used by Coyne. A possible explanation might be that the wires don't contribute significantly to $k_{Cbend}$, but instead the restoring force comes mostly from the copper sheath, and he used a stiffer sheath than we used. However, this is inconclusive, and encourages further investigation.

Finally, Figure 8 suggests strongly of structural damping not only because the straight line through the origin is what is expected for structural damping, but also because Figure 8 is clearly not the alternative – a curve that varied as a function of $f_T^{1/2}$ , as would be expected for velocity damping.

**Conclusion**

Several of LIGO's suspensions need to be fitted with electronics. However, the electronic cabling used to power them may be stiff and heavy, and can potentially degrade the seismic isolation. Experimental characterization of the cabling used in the double pendulum suspension for the OMC concludes that for the pendulum's pitch mode, the cabling exhibits structural damping. For the pitch mode, it is determined that $k_{tor} = 0.005 \pm 0.002$ N-m/rad and $\Phi_C = 0.003 \pm 0.001$, which is constant with respect to $f_T$, the torsional pendulum's pitch mode resonant frequency.

For future work, it would be good to investigate further the previously noted discrepancy between the bending stiffness of our cabling and Coyne's cabling. It would be good to characterize the cabling for the pendulum's yaw and translational motion as well. Also, the cabling model's validity can be further checked by comparing between predicted and measured frequencies of the pendulum with cabling attached. Finally, the model can be used to quantify the isolation degradation of different cabling arrangements.

**Acknowledgments**

I would like to thank my mentors Mark Barton and Norna Robertson for their guidance and support throughout the summer of 2008. I would also like to thank Calum Torrie and Julian Freed-Brown for their help at various points in the project. Last but not least, I would like to thank LIGO, NSF, and Caltech for the wonderful opportunity to work on this project this summer

**References**

1. Barton, M. and Robertson, N, "Understanding Cable Noise in LIGO," http://www.its.caltech.edu/~kgl/ProjectlistPreliminary2008.pdf

2. Rowan, S., "Gravitation Wave Detection by Interferometry," http://relativity.livingreviews.org/Articles/lrr-2000-3/fig02.html

3. "Damping," *Wikipedia*. http://en.wikipedia.org/wiki/Damping

4. Discussion on structural damping with Mark Barton.

5. Coyne D., "Acoustic Coupling through Cabling for the OMC Suspension."